Organic Electronics 13 (2012) 1302–1307

Contents lists available at SciVerse ScienceDirect

Organic Electronics

journal homepage: www.elsevier.com/locate/orgel

CdSe quantum dot cathode buffer for inverted organic bulk hetero-junction solar cells

Yeon-Il Lee, Jun-Ho Youn, Mi-Sun Ryu, Jungho Kim, Jin Jang *

Advanced Display Research Center and Department of Information Display, Kyung Hee University, Dongdaemoon-gu, Seoul 130-701, Korea

ARTICLE INFO

Article history:
Received 11 November 2011
Received in revised form 3 April 2012
Accepted 9 April 2012
Available online 25 April 2012

Keywords:
Organic bulk-heterojunction solar cells
CdSe quantum dot
P3HT
ICBA
Inverted structure

ABSTRACT

A cathode buffer layer made of CdSe quantum dot (QD) is introduced in inverted poly(3-hexylthiophene) (P3HT): Indene-C_{60} Bis-Adduct (ICBA) inverted bulk heterojunction (IBHJ) solar cell. The open-circuit voltage and fill factor increase respectively to 0.88 V and 68.71%, due to the enhanced electron extraction by inserting a CdSe QD layer on Cs_2CO_3/ITO cathode. Thus, the power conversion efficiency increases from 4.6% to 5.2% and the environmental stability is also much improved. By analyzing transmission electron microscope and energy dispersive X-ray spectroscopy, it is found that CdSe QD layer retards Cs diffusion into active layer, leading to improve the lifetime. The ideal temperature dependence of V_{OC} under various illuminations has been achieved with the maximum V_{OC} of 1.205 V.

1. Introduction

Organic solar cells are of increasing interest for renewable energy due to their low cost and low temperature process with printing. Especially, bulk hetero-junction (BHJ) solar cells with a blend of polymer and fullerene derivatives based on solution process are the most promising for flexible, large area applications [1–3]. The conventional BHJ solar cells using regio-regular poly(3-hexylthiophene) (rr-P3HT) and (6,6)-phenyl C_{71} butyric acid methyl ester ($PC_{71}BM$) show the power conversion efficiency (PCE) of 3–5% [3,4] and Li et. al. reported that Indene-C_{60} Bis-Adduct (ICBA) shows the higher V_{OC} of 0.84 V than $PC_{71}BM$ due to the lower level of the lowest unoccupied molecular orbital (LUMO) [5,6].

The environmental stability and lifetime are also important issues for the commercialization of solar cells [7–10]. Recently, the inverted BHJ (IBHJ) solar cells have advantage for long lifetime compared to conventional BHJ solar cells. Control of work function by inserting an interlayer and even convert the polarity of device can be possible. For example, highly efficient P3HT:$PC_{71}BM$ IBHJ solar cell with Cs_2CO_3 and MoO_3 interlayers is demonstrated [11]. Although IBHJ solar cell with alkali metal compound shows the improved performances compared to conventional structure [11,12], Cs atoms can diffuse into active layer and thus degrade the solar cell performance [13].

Colloidal inorganic quantum dots (QD) such as CdSe are usually used as an electron acceptor in various organic photovoltaic cells (OPVs), but power conversion efficiency (PCE) is still low [14,15]. On the other hand, when CdSe QD films are annealed at high temperature, absorption coefficient is reduced and carrier transport is enhanced by the reduction of adjacent distance between individual QDs [16]. Therefore, a CdSe QD layer can be used as an n-type buffer layer in organic IBHJ solar cell.

In this paper, an inverted BHJ solar cell with a CdSe QD buffer layer is demonstrated using solution process. A CdSe QD buffer layer on Cs_2CO_3 improves the performance of inverted solar cells with a P3HT:ICBA active layer. It is found that the existence of CdSe QDs layer can protect Cs-diffusion into active layer, which is confirmed by cross sectional transmission electron microscope (TEM) – energy dispersive X-ray spectroscopy (EDS) analysis. Both cell conversion efficiency and stability can be improved by introducing a thin QD layer in an inverted OPV.

* Corresponding author. Tel.: +82 2 961 0270; fax: +82 2 961 9154.
E-mail address: jjang@khu.ac.kr (J. Jang).

1566-1199/$ - see front matter © 2012 Elsevier B.V. All rights reserved.
http://dx.doi.org/10.1016/j.orgel.2012.04.013

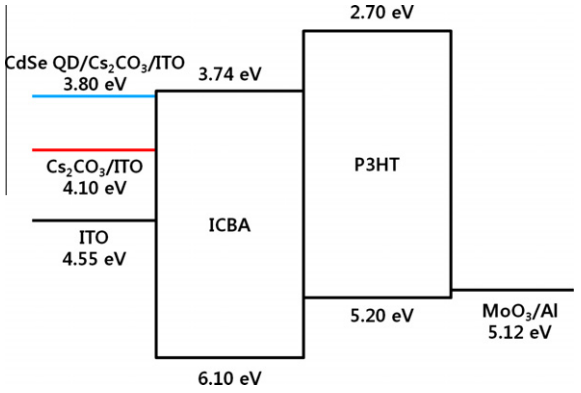

Fig. 1. Device and energy band structures of P3HT:ICBA IBHJ solar cells.

2. Experiment

The device structure studied in this work is an *ITO (150 nm)/Cs_2CO_3*/CdSe QDs/P3HT:ICBA (90 *nm)/MoO_3* (2 *nm)/Al* (100 *nm)* as shown in Fig. 1. The IBHJ solar cells were prepared according to the following procedure. First, a 0.1 wt.% Cs_2CO_3 resolved in 2-ethoxy ethanol was spin coated with 4000 rpm on the patterned ITO glass substrate and the Cs_2CO_3 layer was then annealed at 150 °C for 20 min. CdSe QDs (CdSe 590, QD size: 4.0–4.3 nm, Aldrich) solution dispersed in toluene (5 mg/ml) was spin-casted with 1000 rpm and then annealed.

Then, 1.5 wt.% of P3HT (Aldrich) and ICBA (Lumtec) were separately dissolved in 1,2 dicholorobenzene. Active layer (P3HT:ICBA) is formed using a blended solution with 1:0.6 ratio. The active solutions were spin-casted with 700 rpm and then annealed at 150 °C for 15 min, resulting in ~90 nm, measured by a surface profiler (ET-3000 Kosaka. Lab. Ltd.). And then, 2 nm of MoO_3 layer was evaporated on the active layer with a deposition rate of 0.01 nm/s and then 100 nm of Al layer was deposited in a vacuum of $\sim 10^{-7}$ Torr. Then, the cells were encapsulated with a glass cap and UV-resin to minimize the diffusion of H_2O and O_2 into OPVs. A current meter (Keithley 2400LV) and a solar simulator (MAX-302) were used to measure cell performance under AM 1.5 (100 mW cm^{-2}). External quantum efficiency (EQE) was measured by using a monochromator (Oriel Cornerstone 130) with a 300 W xenon light source.

To monitor the trend of degradation, the solar cells were stored in ambient air at 295 K under ~30% of humidity. The temperature dependence measurements were carried out in a vacuum cryostat system (JANIS CCS-450) of 10^{-3} mbar.

3. Results and discussion

Fig. 2 shows the *J–V* characteristics of the IBHJ cells under illumination. The cell properties of the inverted IBHJ solar cells are summarized in Table 1. PCE of P3HT:ICBA cell increases from 4.6% to 5.2% by inserting a CdSe QD layer annealed at 523 K. Although PCE of P3HT:ICBA IBHJ cell increases by inserting a CdSe QD layer, J_{SC} is nearly the same as that without QD layer. Inserting CdSe QD layer do not affect J_{SC} and external quantum efficiency (EQE), as shown in Fig. 2. Nearly the same EQE indicates that both absorption by a CdSe QD layer and charge transfer between P3HT and CdSe QD are negligible. On the other hand, V_{OC} increases from 0.84 to 0.88 V and FF increases 63.50–68.71%, leading to the increase in PCE. This is due to the lowering of work function of cathode by coating a CdSe QD layer and thus enhanced electron extraction to cathode [17–19]. V_{OC} is mainly determined by the energy offset between HOMO of p-type donor and LUMO of n-type acceptor. When we compared the P3HT:PC_{71}BM and P3HT:ICBA solar cell, the difference in V_{OC}, 0.61 and 0.84 V, is attributed to the difference between LUMOs of n-type donors [5,6,11]. On the other hand, Brabec et al. reports that the cathode with a lower work function induces higher V_{OC} [20].

Fig. 3 shows the ultraviolet photoelectron spectroscopy (UPS) data of three kinds of cathode materials, indicating the shift of 0.45 by Cs_2CO_3 coating on ITO and additional 0.30 eV shift by adding CdSe QD on Cs_2CO_3. Bare ITO is usually used as anode, not cathode, due to relatively high work

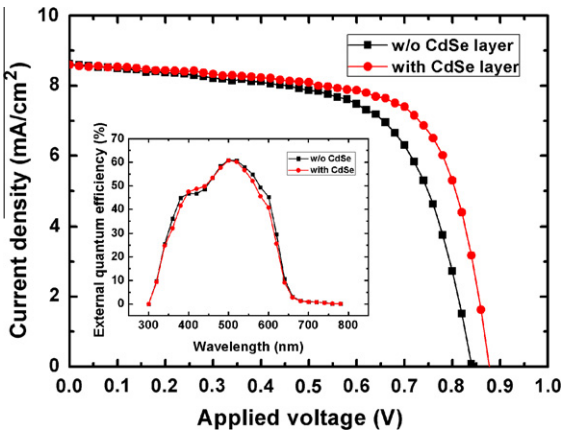

Fig. 2. *J–V* characteristics of P3HT:ICBA IBHJ solar cells under illumination of AM1.5 (100 mW/cm^2). The inset shows the external quantum efficiency of IBHJ solar cells.

Table 1
The best solar cell performances of P3HT:ICBA IBHJ devices with and without a CdSe QD buffer layer. The average value and standard deviation of twelve samples are noted in parenthesis, respectively. R_S is extracted from the slope of *J–V* curve [24].

	V_{OC} (mV)	J_{SC} (mA/cm^2)	FF (%)	PCE (%)	R_s (Ω cm^2)
P3HT:ICBA without CdSe	0.840 (0.832; 0.054)	8.610 (8.302; 0.124)	63.503 (62.812; 0.671)	4.602 (4.352; 0.221)	11.921 (12.522; 0.811)
P3HT:ICBA with CdSe	0.882 (0.881; 0.002)	8.604 (8.574; 0.053)	68.714 (68.142; 0.566)	5.203 (5.171; 0.102)	5.860 (6.120; 0.620)

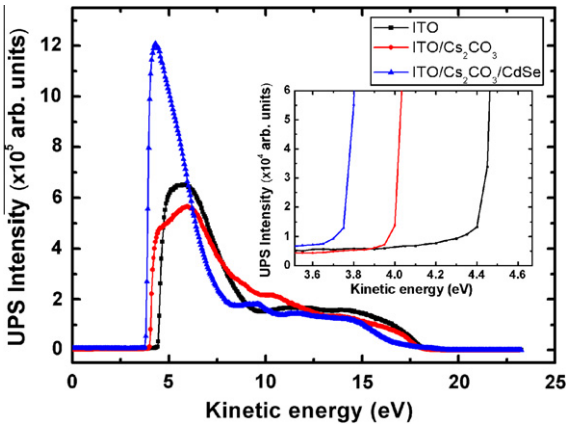

Fig. 3. The UPS data of three kinds of cathodes. The inset shows the expansion of secondary cut-off region to indicate the vacuum level shifts. While, the UPS curves in cut-off region are overlapped at relatively low intensity. We calculated the work functions after compensation by Fermi level of gold.

function. However, Liao et al. report that the effective work function of ITO decreases by the incorporation of Cs_2CO_3 [12]. In our measurement, solution processed Cs_2CO_3 interlayer decreases the work function of ITO from 4.55 to 4.10 eV and thus can be used for inverted configuration with MoO_3/Al anode (5.12 eV). The hybrid interlayer composed of CdSe QD and Cs_2CO_3 layers decreases work function of cathode to 3.8 eV. Well-matched energy level between CdSe QD and ICBA, and high electron mobility of CdSe QD layer leads to higher V_{OC} of 0.88 V and reduce series resistance as shown in Table 1[18–20]. Therefore, V_{OC} and FF of inverted cells increase by inserting a CdSe QD layer.

Typically, colloidal CdSe QDs are capped with polymer ligand such as hexadecylamine. This improves the stability of organic solvent but acts as a potential barrier between QDs in film. Therefore, the electrical resistivity of pristine spherical CdSe QD layer is quite high. Therefore, the device with CdSe QD without annealing shows poor performance

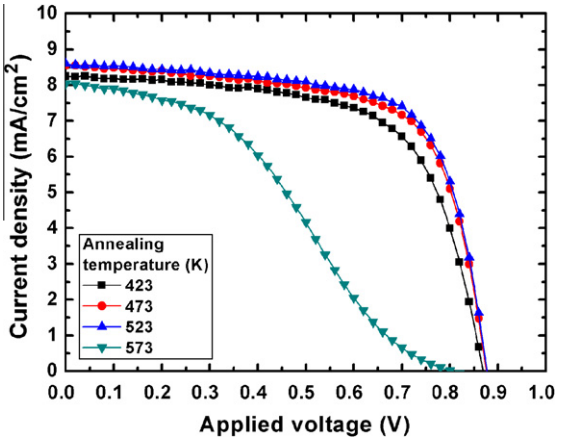

Fig. 4. *J–V* characteristics of P3HT:ICBA IBHJ solar cells with CdSe QD layer which is annealed in temperature range between 423 and 573 K.

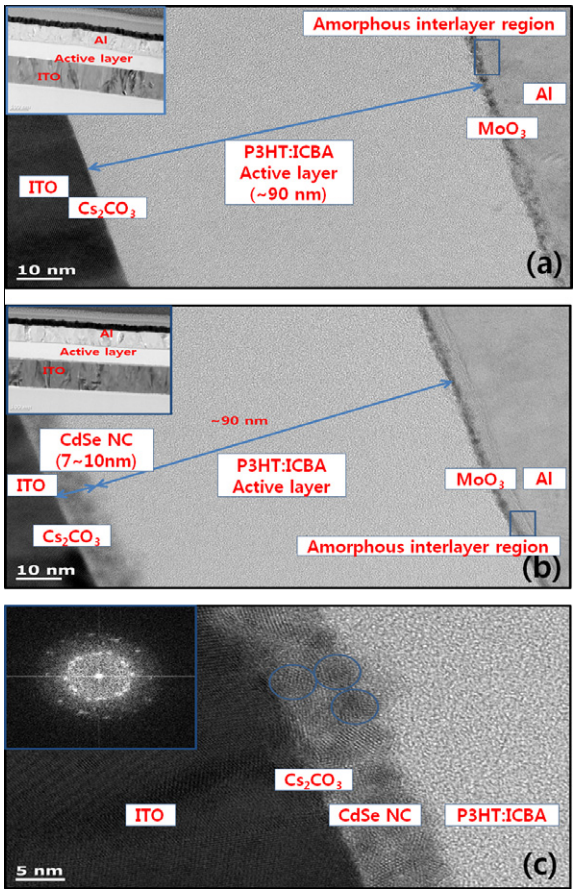

Fig. 5. TEM image of cross-section of P3HT:ICBA IBHJ solar cells; (a) the solar cell without CdSe QD layer, (b) the solar cell with CdSe QD layer, (c) expanded image of CdSe QD layer interface. Circles indicate the QD size and inset shows the XRD pattern of CdSe QDs in circles.

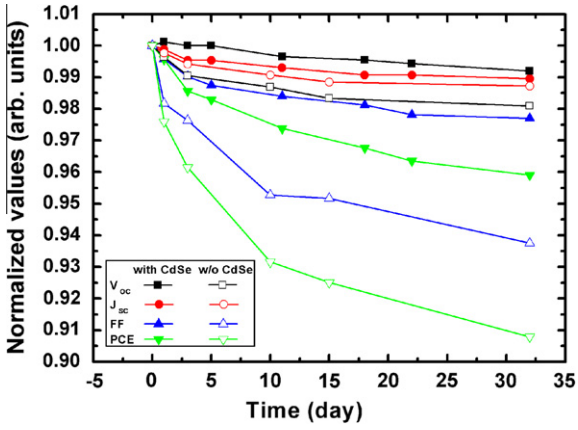

Fig. 6. Variations of solar cell parameters of P3HT:ICBA solar cells with and without CdSe QD layer for 1 month in ambient air condition. To exclude the external factors such as infiltration of H_2O and O_2, cells are encapsulated by glass cap with UV resin.

of V_{OC} = 0.85 V, J_{SC} = 8.11, FF = 57.8% and PCE = 3.98%. However, Drndic et al. report that thermal annealing improves

the carrier transport in CdSe QD layers [16]. They measured the increase of currents and observed the decrease of average distance between QDs by annealing. In addition, Yu et al. reports that the shrunk CdSe QD layer has high electron mobility of $>10^{-2}\,cm^2\,V^{-1}\,s^{-1}$ [21]. Therefore, the performance of IBHJ solar cells with a CdSe QD layer depends on annealing temperature.

Fig. 4 shows the *J–V* characteristics under illumination for the IBHJ cells with a CdSe QD layer annealed in between 423 and 573 K. Thickness of pristine CdSe QD layer is measured to be ~15 nm by a surface profiler. Annealing induces the shrinkage of a coated CdSe QD layer and thus enhances carrier transport. However, annealing at 573 K would damage Cs_2CO_3/ITO. Note that 523 K was used for annealing for the OPV in this work. Inverted cell structure is more suitable for application of QD as an n-type buffer which requires annealing at >500 K.

Fig. 5 shows the cross sectional TEM images; (a) OPV without QD layer, (b) OPV with CdSe QD layer of 7–10 nm, (c) expanded CdSe QD region in (b). The CdSe QD layer was annealed at 523 K. The distance between QDs is very close and about two QD stack layer leads to 7–10 nm. The diameter of a CdSe QD is ~4 nm from (c). Inset of Fig. 5c shows the X-ray diffraction pattern of a CdSe QD layer indicating crystalline structure.

IBHJ solar cells with a hybrid n-type interlayer have a merit in environment stability. By using a Cs_2CO_3 buffer layer in OPV, Cs-diffusion can induce degradation of solar cells [13]. The degradation of P3HT:PC_{71}BM IBHJ solar cells with a Cs_2CO_3 layer is reported; initial degradation is dominated by the rapid decrease of V_{OC} and FF, showing exponential decay [11]. The reduction of FF and V_{OC} is also dominant factor for degradation of P3HT:ICBA IBHJ solar cell without a CdSe QD layer. On the other hand, V_{OC} of P3HT:ICBA IBHJ solar cell with a CdSe QD layer maintains 99% of an initial value during 1 month and decreasing rate of FF decreases also as shown Fig. 6. Consequently, PCE of P3HT:ICBA IBHJ solar cell decreases to 96% of an initial value in 1 month in ambient air.

The Cs-diffusion in active layer in IBHJ cell can be seen in TEM-EDS analysis as shown in Fig. 7 and Table 2. The IBHJ solar cells were stored in air condition for 100 days. EDS data on P3HT:ICBA IBHJ solar cells without CdSe QD layer indicate that Cs could diffuse to position 4

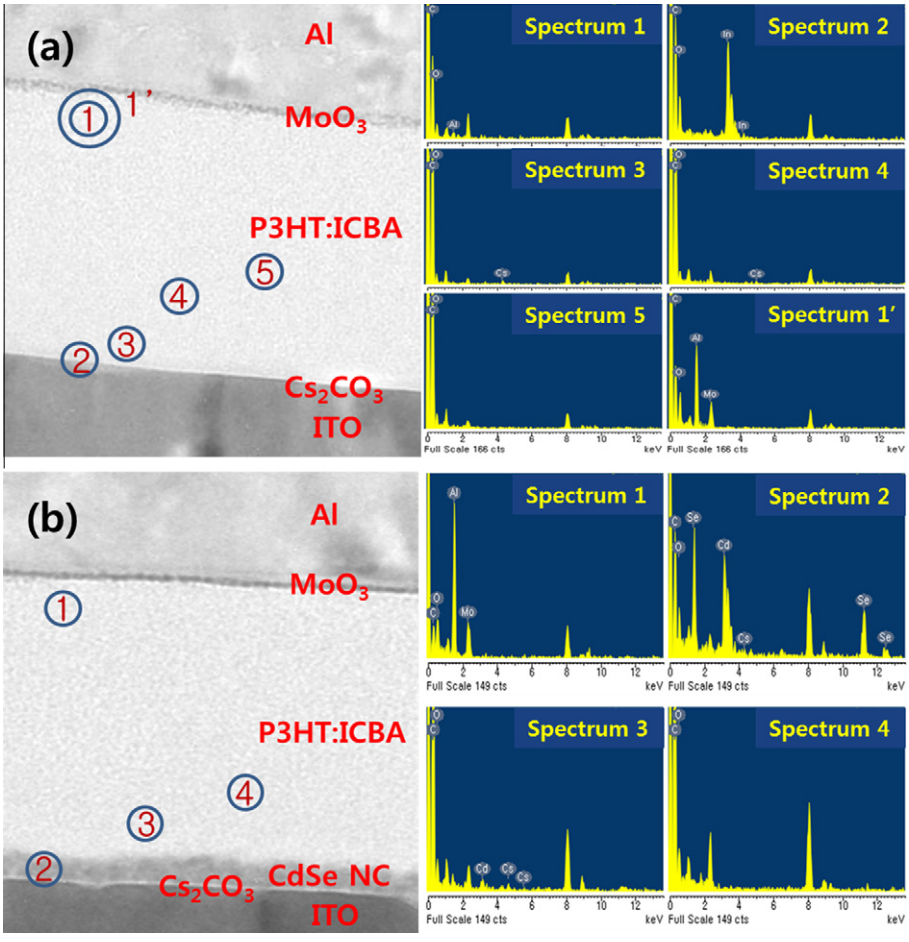

Fig. 7. The EDS data of IBHJ solar cells (a) without CdSe QD layer and (b) with CdSe QD layer. The left indicates the detecting positions. Cs near the ITO (position 2 in sample without CdSe) is difficult to distinguish due to high intensity of In. The circles indicate the beam incident area with ~10 nm of beam spot size except 1′ (~15 nm). The summary is shown in Table 2.

Table 2
The TEM-EDS analysis data of P3HT:ICBA IBHJ solar cells; (a) without CdSe QD layer and (b) with CdSe QD layer. This table indicates all the elements at each position in atomic%. The positions are shown in Fig. 7. The EDS beam spot size is ~10 nm except position 1′ (~15 nm).

Without CdSe	C	O	Al	Mo	In	Cs
Position 1	87.26	11.04	1.70	0	0	0
Position 2	68.72	17.78	0	0	13.50	0
Position 3	96.68	3.06	0	0	0	0.26
Position 4	98.15	1.71	0	0	0	0.14
Position 5	97.87	2.13	0	0	0	0
Position 1′	58.74	19.12	20.56	1.58	0	0

With CdSe	C	O	Al	Se	Mo	Cd	Cs
Position 1	91.67	8.33	0	0	0	0	0
Position 2	67.90	10.54	0	8.97	0	11.85	0.74
Position 3	97.81	1.84	0	0	0	0.20	0.14
Position 4	98.14	1.86	0	0	0	0	0

(~25.4 nm depth) in the active layer. On the other hand, in device with CdSe QD layer, Cs components are detected until position 3 (~13.2 nm depth). The atoms such as Mo, Al, Cd, Se are quite stable because of the large sizes. For example, Mo is hardly detected at position 1 (spectrum 1). When we used the larger beam spot size (spectrum 1′) which reaches to the boundary of MoO_3 layer, the Mo and Al elements were detected. Therefore, Cs-diffusion would induce the degradation of IBHJ solar cells and the additional buffer layer of CdSe QD layer is able to retard the alkali metal diffusion to active layer.

We also investigated the temperature dependence of V_{OC} under various illumination intensities. The V_{OC} of organic photovoltaic cells originates from the energy offset in active layer. However, V_{OC} is reduced by lowering chemical potential at the interface or phonon scattering during the transport process. At specific temperature, V_{OC} increases logarithmically with increasing the illumination intensity and increases linearly with decreasing temperature. Fig. 8 shows the V_{OC} versus temperature at various illumination intensities. In the temperature range between

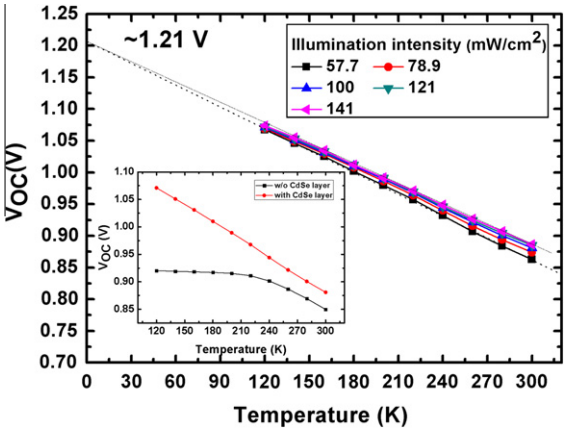

Fig. 8. The plot of the temperature dependence of V_{OC} in P3HT:ICBA IBHJ solar cell with CdSe QD layers with varying illumination intensities. Inset shows the V_{OC}–T curves of P3HT:ICBA IBHJ solar cell with and without a CdSe QD layer.

120 and 300 K, the slope of V_{OC} curve shows linear dependence which indicates the less loss of V_{OC} during carrier extraction. It decreases gradually with increasing illumination intensity and extrapolated V_{OC} curves are ideally converged near 0 K. We found that the maximum V_{OC} of P3HT:ICBA system is 1.21 V using Eq. (1),

$$V_{OC} \sim \frac{E_g}{q} - \frac{nkT}{q} \ln\left(\frac{N_V N_C \mu kT}{J_{SC} L N_A}\right), \quad (1)$$

where E_g is the band gap of absorption material in classic PN solar cell [22,23]. In organic BHJ solar cells, it corresponds to the off-set between the HOMO of p-type donor material and LUMO of n-type acceptor material. The offset between HOMO of P3HT and LUMO of ICBA is close to the measured maximum value of V_{OC}. Comparing the maximum V_{OC} (0.965 V) of P3HT:PC_{71}BM solar cells, the LUMO level of ICBA appears to be ~0.240 eV higher than that of PC_{71}BM due to the same usage of P3HT [11].

Linear relationship between V_{OC} and temperatures indicates the ideal energy level matching between cathode and LUMO of n-type acceptor. As the work function of cathode decreases until LUMO of n-type acceptor, V_{OC} increases gradually. If the work function of the cathode is lower than LUMO of n-type acceptor, a potential barrier exists for electron extraction. Therefore, LUMO of n-type acceptor is the upper limit of cathode for optimized electron extraction without the electrical energy loss.

4. Conclusion

We studied the effect of CdSe QD interlayer on the P3HT:ICBA IBHJ solar cell. Inserting CdSe QD layer on Cs_2CO_3/ITO cathode decreases the work function of cathode and reduces the series resistance. Therefore, V_{OC} increases from 0.840 to 0.882 V, FF increases from 63.5 to 68.7 and PCE increases also from 4.61% to 5.20%. Note that short circuit current density is almost the same. Insertion of CdSe QD layer retards the Cs-diffusion into the active layer and thus improve the lifetime of IBHJ cells, which is confirmed by TEM-EDS analysis. In addition, the maximum V_{OC} of P3HT:ICBA cells can be 1.205 V at 0 K.

Acknowledgements

This work was supported by Korea Science & Engineering Foundation through the Nano Technology Development Program (Grant No. 2007-02775).

References

[1] G. Yu, J. Gao, J.C. Hummelen, F. Wudl, A.J. Heeger, Science 270 (1995) 1789.
[2] C.J. Brabec, Sol. Energy Mater. Sol. Cells 83 (2004) 273.
[3] S.E. Shaheen, C.J. Brabec, N.S. Sariciftci, F. Padinger, T. Fromherz, J.C. Hummelen, Appl. Phys. Lett. 78 (2001) 841.
[4] J.J.M. Halls, C.A. Walsh, N.C. Greenham, E.A. Marseglia, R.H. Friend, S.C. Moratti, A.B. Holmes, Nature 376 (1995) 498.
[5] Y. He, H.-Y. Chen, J. Hou, Y. Li, J. Am. Chem. Soc. 132 (2010) 1377.
[6] G. Zhao, Y. He, Y. Li, Adv. Mater. 22 (2010) 4355.
[7] F.C. Krebs, J. Fyenbo, D.M. Tanenbaum, S.A. Gevorgyan, R. Andriessen, B.V. Remoortere, Y. Galagan, M. Jorgensen, Energy Environ. Sci. 4 (2011) 4116.
[8] S.A. Gevorgyan, A.J. Medford, E. Bundgaard, S.B. Sapkota, H.F. Schleiermacher, B. Zimmermann, U. Wurfel, A. Chafiq, M. L-Cantu,

T. Swonke, M. Wagner, C.J. Brabec, O. Haillant, E. Voroshazi, T. Aernouts, R. Steim, J.A. Hauch, A. Elschner, M. Pannone, M. Xiao, A. Langzettel, D. Laird, M.T. Lloyd, T. Rath, E. Maier, G. Trimmel, M. Hermenau, T. Menke, K. Leo, R. Rosch, M. Seeland, H. Hoppe, T.J. Nagle, K.B. Burke, C.J. Fell, D. Vak, T.B. Singh, S.E. Watkins, Y. Galagan, A. Manor, E.A. Katz, T. Kim, K. Kim, P.M. Sommeling, W.J.H. Verhees, S.C. Veenstra, M. Riede, M.G. Christoforo, T. Currier, V. Shrotriya, G. Schwartz, F.C. Krebs, Sol. Energy Mater. Sol. Cells. 95 (2011) 1398–1416.

[9] M. Jorgensen, K. Norrman, F.C. Krebs, Sol. Energy Mater. Sol. Cells. 92 (2008) 686–714.

[10] M.O. Reese, S.A. Gevorgyan, M. Jorgensen, E. Bundgaard, S.R. Kurtz, D.S. Ginley, D.C. Olson, M.T. Lolyd, P. Morvillo, E.A. Katz, A. Elschner, O. Haillant, T.R. Currier, V. Shrotriya, M. Hermenau, M. Riede, K.R. Kirov, G. Trimmel, T. Rath, O. Inganas, F. Zhang, M. Andersson, K. Vingstedt, M.L. Cantu, D. Laird, C. McGuiness, S.J. Gowrisaner, M. Pannone, M. Pannone, M. Xiao, J. Hauch, R. Steim, D.M. Delongchamp, R. Rosch, H. Hoppe, N. Espinosa, A. Urbina, G.-Y. Uzunoglu, J.-B. Bonekamp, A.J.J.M.V. Breemen, C. Girotto, E. Voroshazi, F.C. Krebs, Sol. Energy Mater. Sol. Cells. 95 (2011) 1253–1267.

[11] Y.-I. Lee, J.-H. Youn, M.-S. Ryu, J. Kim, H.-T. Moon, J. Jang, Org. Electron. 12 (2011) 353.

[12] H.-H. Liao, L.-M. Chen, Z. Xu, G. Li, Y. Yang, Appl. Phys. Lett. 92 (2008) 173303.

[13] C.-C. Hsiao, A.-E. Hsiao, S.-A. Chen, Adv. Mater. 2008 (1982) 20.

[14] N.T.N. Truong, W.K. Kim, C. Park, Sol. Ener. Mater. & Sol. Cell. 95 (2011) 167.

[15] S. Dayal, N. Kopidakis, D.C. Olson, D.S. Ginley, G. Rumbles, Nano Lett. 10 (2010) 239.

[16] M. Drndic, M.V. Jarosz, N.Y. Morgan, M.A. Kastner, M.G. Bawendi, J. Appl. Phys. 92 (2002) 7498.

[17] F. Zhang, M. Ceder, O. Inganas, Adv. Mater. 19 (2007) 1835–1838.

[18] S.A. Carter, M. Angelopoulos, S. Karg, P.J. Brock, J.C. Scott, Appl. Phys. Lett. 70 (1997) 2067.

[19] C.J. Barbec, S.E. Shaheen, C. Winder, N.S. Sariciftci, P. Denk, Appl. Phys. Lett. 84 (2004) 3906.

[20] C.J. Brabec, A. Cravino, D. Meissner, N.S. Sariciftci, T. Fromherz, M.T. Rispens, L. Sanchez, J.C. Hummelen, Adv. Funct. Mater. 11 (2001) 374.

[21] D. Yu, B.L. Wehrenberg, P. Jha, J. Ma, P. Guyot-Sionnest, J. Appl. Phys. 99 (2006) 104315.

[22] F.C. Chen, J.L. Wu, S.S. Yang, K.H. Hsieh, W.C. Chen, J. Appl. Phys. 103 (2008) 103721.

[23] I. Riedel, J. Parisi, V. Dyakonov, L. Lutsen, D. Vanderzande, J.C. Hummelen, Adv. Funct. Mater. 14 (2004) 38.

[24] T. Aernouts, W. Geens, J. Poortmans, P. Heremans, S. Borghs, R. Mertens, Thin Solid Films 403–404 (2002) 297.